S8 Time Series Analysis

Ed Cohen

Room: 536 Huxley

email: e.cohen@imperial.ac.uk

Use Blackboard to obtain all course resources

Department of Mathematics

Imperial College London

180 Queen's Gate, London SW7 2BZ

With thanks to Prof Andrew Walden

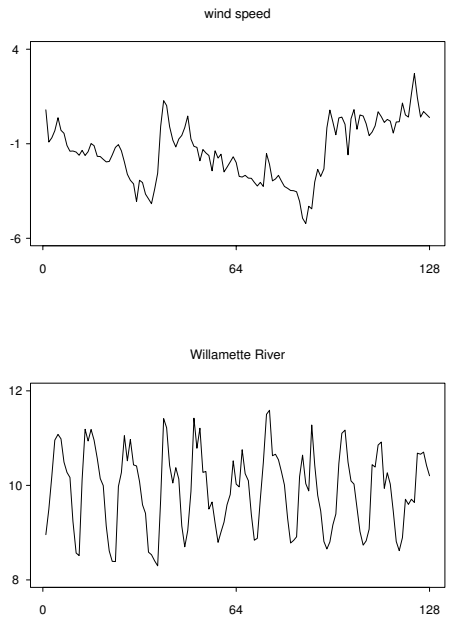

Figure 1: Plots of portions of the first two time series. For both time series the vertical axis is the value of the time series (in unspecified units), while the horizontal axis is time (measured at 0.025 second intervals for the wind speed series and in months for the Willamette River series).

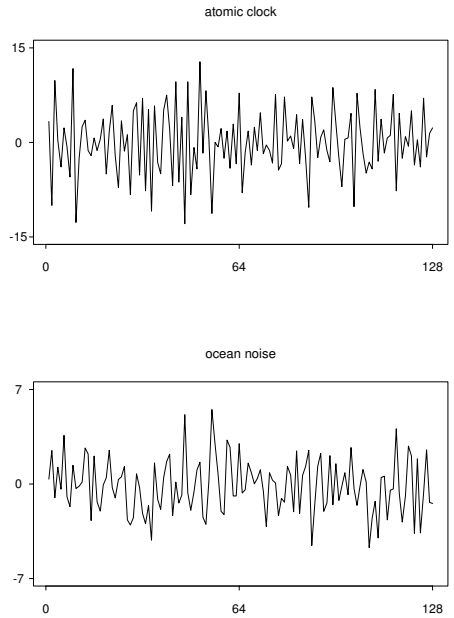

Figure 2: Plots of portions of the next two time series. The horizontal axes are again time (measured in days for the atomic clock series and in seconds for the ocean noise series).

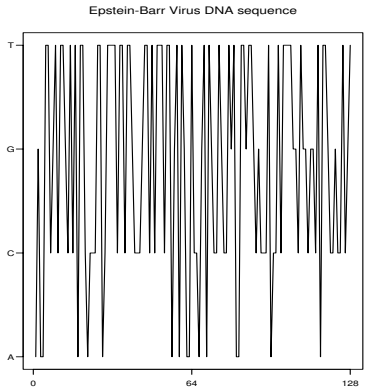

Figure 3: Plot of a portion of the epstein-Barr Virus DNA sequence, made up of the four different bases (bp), thymine (**T**), cytosine (**C**), adenine (**A**) and guanine (**G**). The full EBV DNA sequence consists of approximately 172,000 bp.

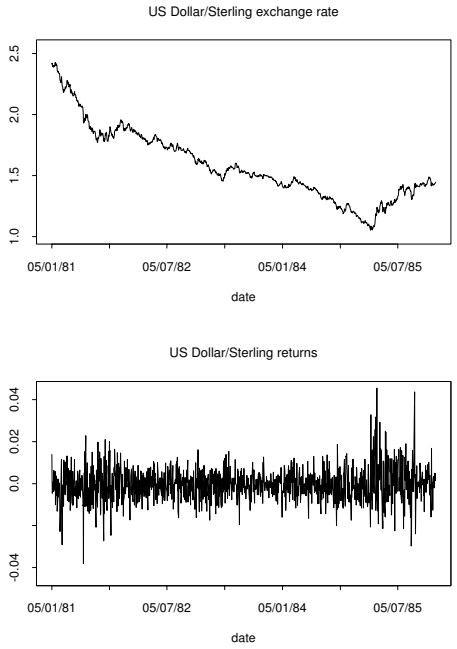

Figure 4: Plots of the US Dollar/Sterling exchange rate from 05/01/81 to 31/12/85 and the associated returns. The horizontal axes are again time (measured in days).

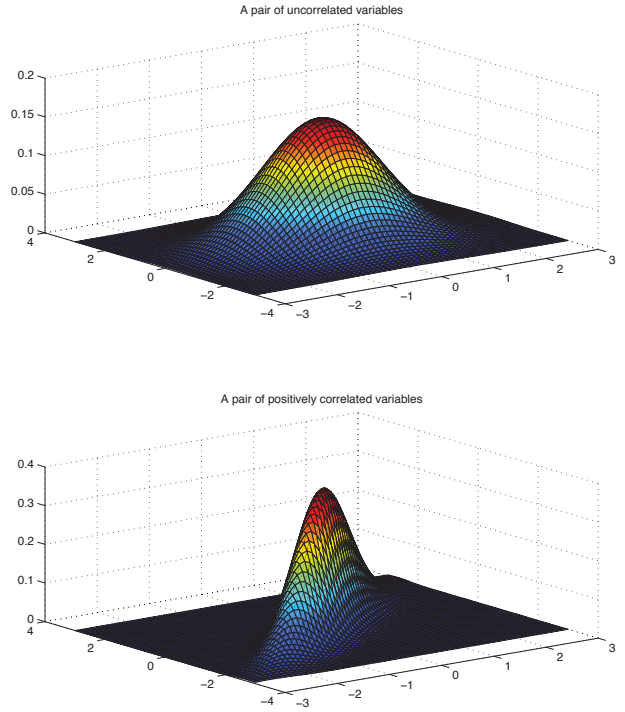

Figure 4a: Bivariate pdfs for two random variables which are uncorrelated (top) or positively correlated (bottom). Bivariate normal distribution used.

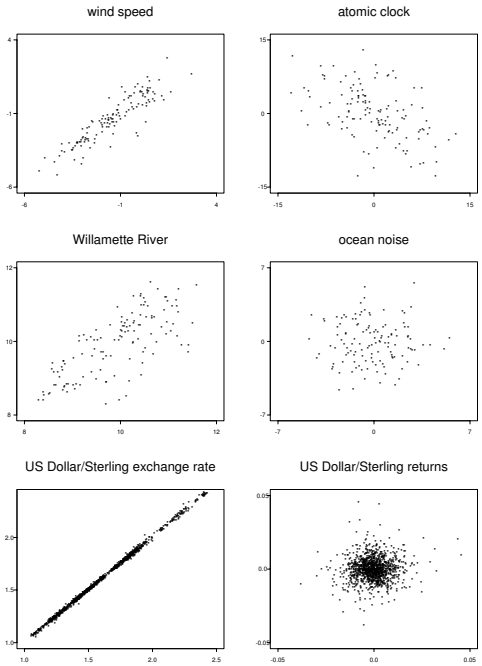

Figure 5: Lag 1 scatter plots for the time series in Figures 1, 2, and 4. In each of these plots, the values of the times series at time $t+1$ is plotted on the vertical axis versus the value at time t on the horizontal axis.

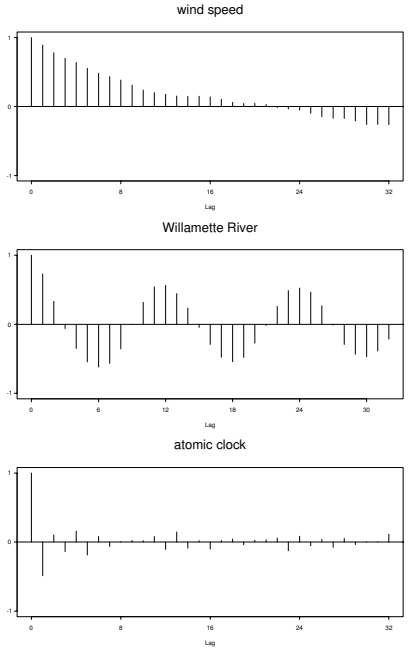

Figure 6: Sample autocorrelations for the time series.

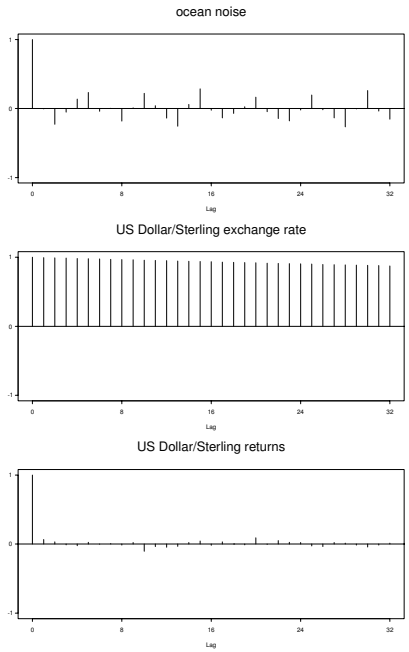

Figure 7: Sample autocorrelations for the time series.

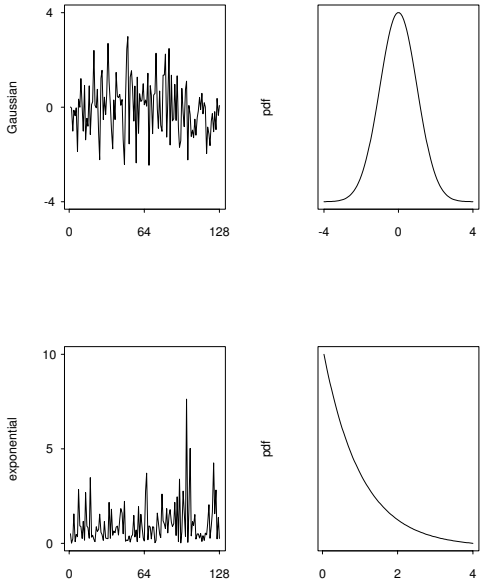

Figure 8: Realizations of two white noise processes and their underlying densities. The distribution for the process in the top left plot is Gaussian (with mean zero and variance 1), while the one for the bottom left plot is Chi-squared with two degrees of freedom (exponential) – this distribution is one-sided (i.e., an rv with this distribution can assume only nonnegative values) and has a heavier tail than the Gaussian distribution. This gives the time series the appearance of having outliers.

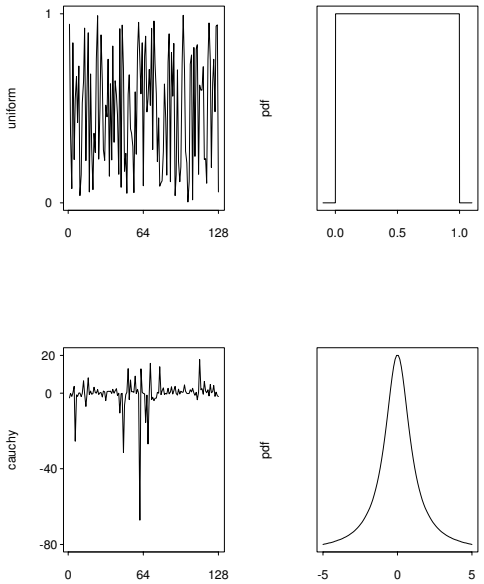

Figure 9: Realizations of two more white noise processes and their underlying densities. The distribution for the process in the top left plot is uniform on the interval $[0, 1]$, while the one for the bottom left plot has a Cauchy distribution that has been truncated at $\pm 10^{10}$ to produce a distribution with finite mean and variance – a requirement for second-order stationarity. The tails fo the truncated Cauchy distribution are heavier than for both distributions in Figure 8, while the tails for the uniform distribution are lighter.

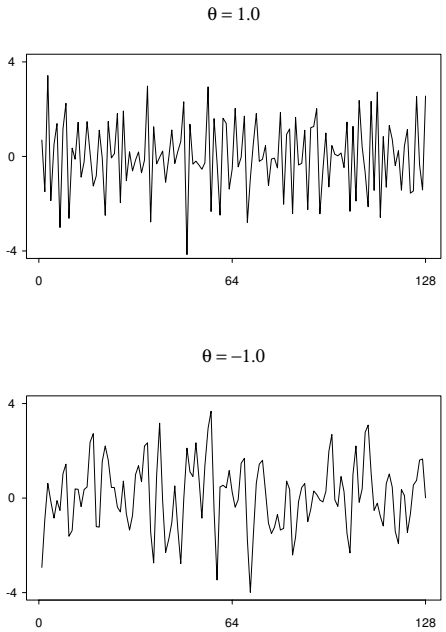

Figure 10: Realizations of size 128 of two first-order Gaussian moving average processes. The top and bottom plots are for processes with $\theta = 1.0$ and $\theta = -1.0$ respectively, and $\sigma_\epsilon^2 = 1.0$ in both cases.

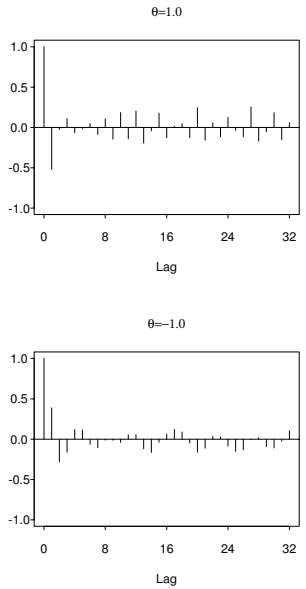

Figure 11: Sample acs for the MA(1) processes shown in Figure 10.

Theoretical acs is given by:

$\rho_0 = 1.0, \rho_1 = -0.5$, when $\theta_{1,1} = 1.0$

$\rho_0 = 1.0, \rho_1 = 0.5$, when $\theta_{1,1} = -1.0$

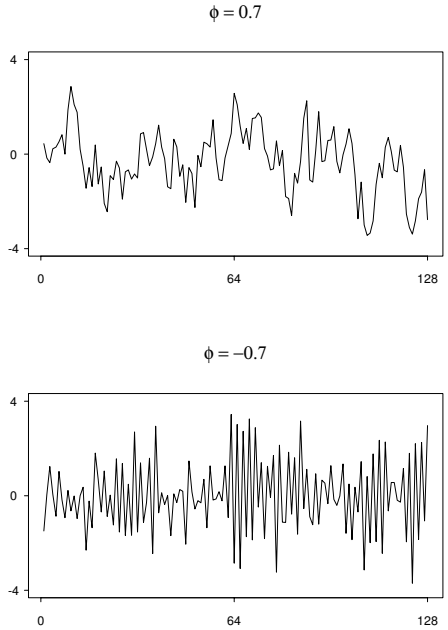

Figure 12: Realizations of size 128 of two first-order Gaussian autoregressive processes. The top and bottom plots are for processes with $\phi = 0.7$ and $\phi = -0.7$ respectively, and $\sigma_\epsilon^2 = 1.0$ in both cases. ($\phi = \phi_{1,1}$).

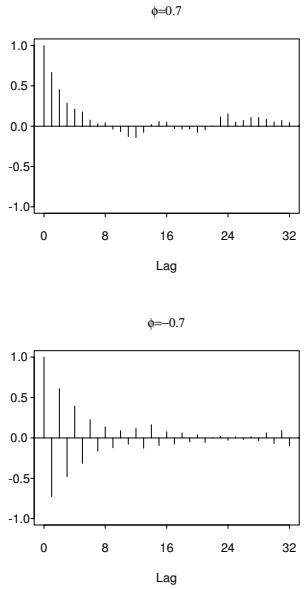

Figure 13: Sample acs for the AR(1) processes shown in Figure 12.

Theoretical acs is given by:

$\rho_\tau = \phi_{1,1}^{|\tau|}, \quad \tau = 0, \pm 1, \pm 2, \ldots.$

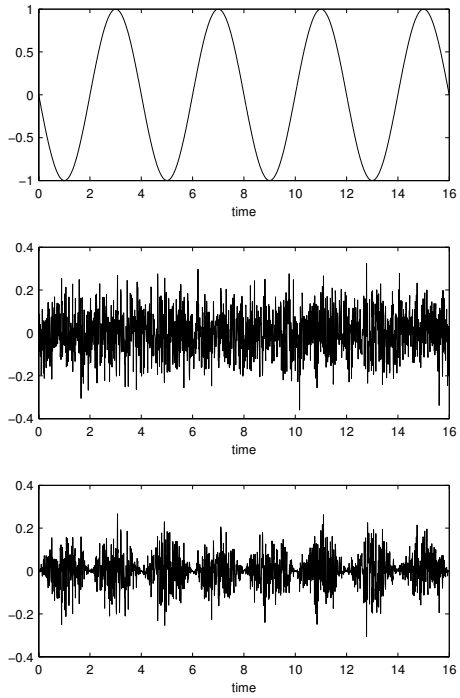

Figure 14: Top plot: $\cos(2\pi f_0 t + \phi)$, with $\phi = \frac{\pi}{2}$, and $f_0 = 0.25$.

Middle plot: simulated random normal process $\{\epsilon_t\}$, with $\sigma_\epsilon = 0.1$.

Bottom plot: simulated harmonic process, $X_t = \epsilon_t \cos(2\pi f_0 t + \phi)$.

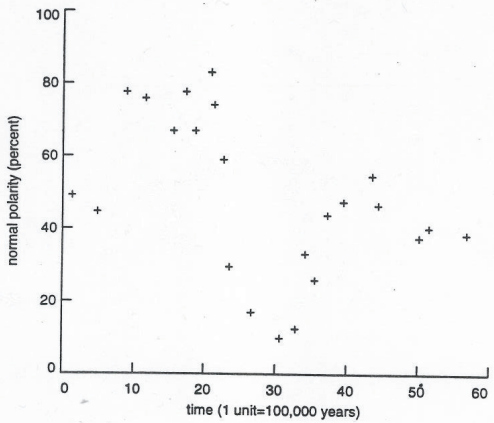

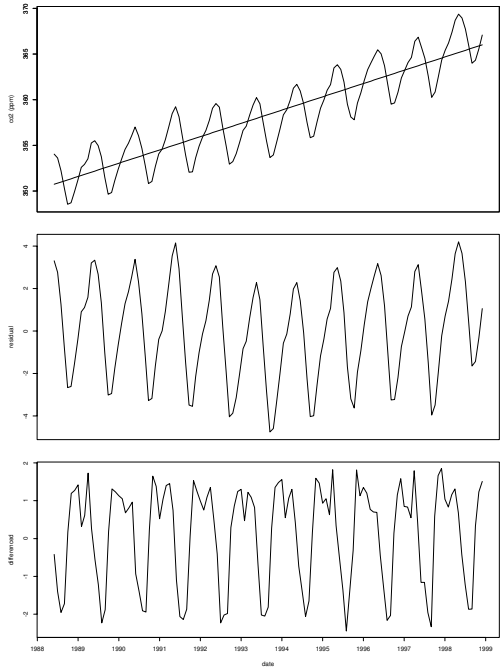

Figure 15: Top plot: Atmospheric CO_2 concentrations (ppmv) derived from in situ air samples collected at Mauna Loa Observatory, Hawaii. The least squares straight line fit is also shown. Source: Keeling & Whorf, Scripps Institution of Oceanography (SIO), University of California.
Middle plot: the residuals from the least squares fit.
Bottom plot: the first differences.

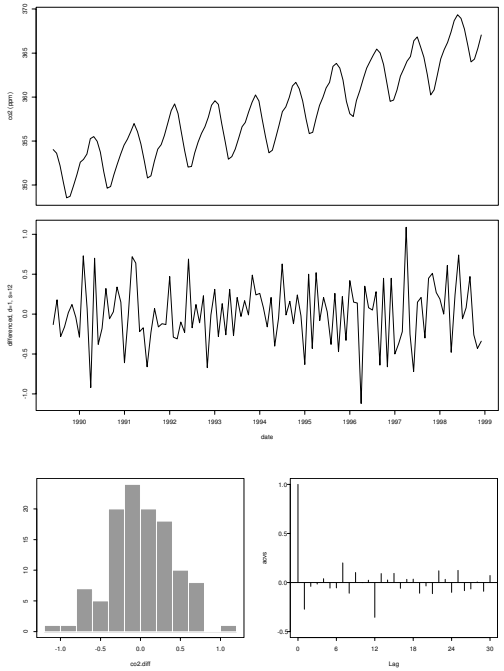

Figure 16: Top plot: X_t: Atmospheric CO_2 concentrations (ppmv).

Source: Keeling & Whorf, Scripps Institution of Oceanography (SIO), University of California.

Middle plot: first differences, followed by lag 12 differening.

i.e. applying $Y_t = (1 - B^s)(1 - B)X_t$ with $s = 12$.

Bottom plot (left) histogram of Y_t.

Bottom plot (right) acvs of Y_t.

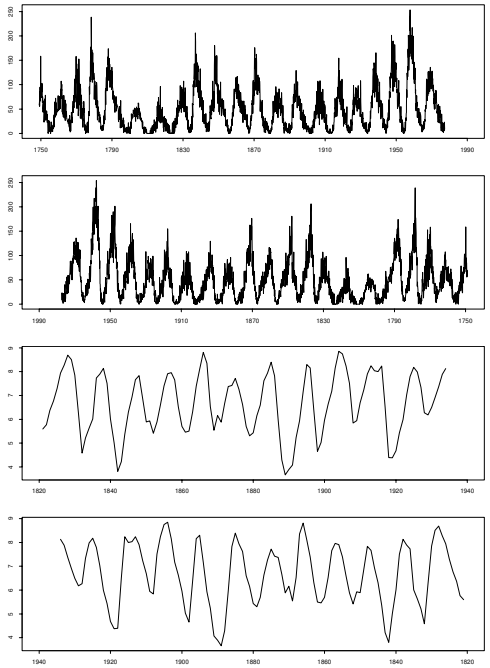

Figure 17: Top two plots: The monthy sunspot numbers (1749 to 1977) in forward and reverse time – note that the values rise more rapidly than they fall.

Bottom two plots: the yearly log Canadian lynx data (1821 to 1934) – again the values rise more rapidly than they fall.